

36. All experiments involving animals were conducted under protocols approved by the Institutional Animal Care and Use Committee of Abbott Laboratories. The authors acknowledge the synthetic contributions of J. Lynch, J. Wasicak, and H. Bai; the biological contribu-

tions of D. Anderson and D. J. B. Kim; and J. Daly for his pioneering work in the field and his thoughtful input to this manuscript.

12 September 1997; accepted 11 November 1997

## Inhibition of the Hammerhead Ribozyme Cleavage Reaction by Site-Specific Binding of Tb(III)

Andrew L. Feig, William G. Scott, Olke C. Uhlenbeck\*

Terbium(III) [Tb(III)] was shown to inhibit the hammerhead ribozyme by competing with a single magnesium(II) ion. X-ray crystallography revealed that the Tb(III) ion binds to a site adjacent to an essential guanosine in the catalytic core of the ribozyme, approximately 10 angstroms from the cleavage site. Synthetic modifications near this binding site yielded an RNA substrate that was resistant to Tb(III) binding and capable of being cleaved, even in the presence of up to 20 micromolar Tb(III). It is suggested that the magnesium(II) ion thought to bind at this site may act as a switch, affecting the conformational changes required to achieve the transition state.

RNA enzymes require divalent metal ions for activity, either to promote folding or for direct participation in catalysis. The hammerhead ribozyme (Fig. 1A), a self-cleaving RNA found naturally in plant viroids and virusoids, is an excellent system in which to study metal ion-RNA interactions because of the extensive structural and mechanistic data available (1-4). Two independent crystal structures of the hammerhead ribozyme have revealed divalent metal ions binding to six different sites on the molecule (5-7). Biochemical methods available to evaluate the role of these metal ions in ribozyme function are limited. The most common approach is to introduce a phosphorothioate modification into the RNA and to examine its effect on the metal specificity of the catalytic reaction (8-13). We present an approach to studying metal binding to ribozymes based on the observation that ions that compete efficiently for critical Mg-binding sites can thereby inhibit catalysis. The powerful enzymatic and spectroscopic tools originally developed for use with protein metalloenzymes can then be applied to RNA systems such as the hammerhead ribozyme.

Interactions between lanthanide ions and RNA molecules have been studied (14, 15). The luminescence properties of Tb(III) made it an attractive choice from a list of potential inhibitors (16). Irradiation (excitation wavelength, 260 nm) of a 1  $\mu$ M solution of ham-

merhead 16 (HH16) (17) in the presence of 10  $\mu$ M Tb(III) and 10 mM Mg(II) resulted in sensitized emission from the  $^3D_4$  state of the Tb ion (Fig. 1B). This signal was absent from control samples lacking either RNA or Tb(III). These data indicate that the Tb ion binds to the RNA, resulting in energy transfer from the RNA to the lanthanide ion. We therefore investigated the effects of Tb(III) binding on the hammerhead-catalyzed reaction, a site-specific cleavage of a phosphodiester bond to form 2',3'-cyclic phosphate and 5'-hydroxyl termini.

Terbium(III) proved an efficient inhibitor of hammerhead cleavage (18). For example, Tb(III) inhibited the HH8 single-turnover cleavage reaction with an apparent inhibition constant ( $K_{i,app}$ ) of  $2.0 \pm 0.3 \mu$ M at 25 mM Mg(II) (Fig. 2A), and similar values were obtained under multiple-turnover conditions. Two other well-characterized hammerheads, HH16 (19) and HH $\alpha$ 1 (20), showed  $K_{i,app}$  values for Tb(III) of  $1.1 \pm 0.4$  and  $0.57 \pm 0.08 \mu$ M, respectively, at 10 mM Mg(II) (21). Because all three ribozymes were inhibited similarly by Tb(III) despite sequence differences in the peripheral base-paired regions and loops, the data indicate that the binding event that underlies inhibition results from the interaction of Tb(III) with a site in the conserved catalytic core.

The  $K_{i,app}$  values for Tb(III) increased with increasing Mg(II) concentrations, indicating that the two ions compete for a site (Fig. 2B). Competition was confirmed by a chase experiment (Fig. 2C); when Tb(III) was added to a cleavage reaction after it had already started, the reaction stopped rapidly and completely. When even higher concentrations of Mg(II) were later added to the

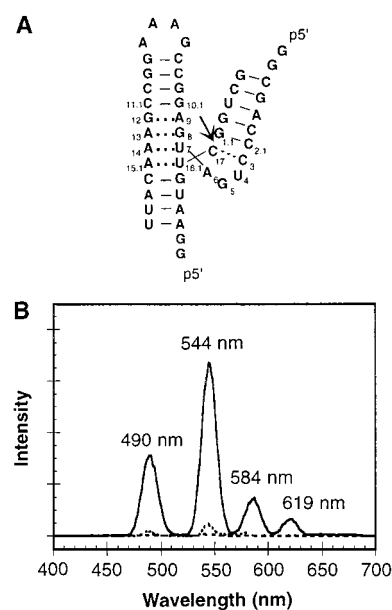


**Fig. 1.** (A) Schematic representation of the hammerhead ribozyme as well as the standard numbering scheme for the residues (38). The sequence shown is that of hammerhead 8 (HH8), a construct that has been previously characterized (39) and was used for most of the inhibition studies. (B) Sensitized luminescence spectrum of 10  $\mu$ M TbCl<sub>3</sub> in the presence of 10 mM MgCl<sub>2</sub> and 1  $\mu$ M HH16 (solid line). Control luminescence spectra of 1  $\mu$ M HH16 and 10 mM MgCl<sub>2</sub> with no added TbCl<sub>3</sub> and of 100  $\mu$ M TbCl<sub>3</sub> in water (dashed and dotted lines, respectively) are also shown. Excitation was at 260 nm.

same reaction, cleavage resumed. The reversibility of this inhibition implied that the Tb(III) adduct rapidly equilibrates with the fully hydrated ion and does not irreversibly damage the hammerhead. This implication was confirmed by direct analysis of the RNA by gel electrophoresis after incubation with Tb(III) for up to 4 hours (22).

Two crystallographic experiments were performed to determine the location of Tb(III) binding. In one experiment, 2 mM TbCl<sub>3</sub> was allowed to soak into already-formed crystals of the hammerhead; in the other, the ribozyme was crystallized in the presence of 2 mM TbCl<sub>3</sub> (Table 1). The high concentration was required to offset the ionic strength of the mother liquor. In both instances, the overall structures were identical to the native hammerhead with the exception of localized regions of positive electron density indicative of metal binding. The difference electron density map from the cocrystallization experiment (Fig. 3A) revealed three bound ions. The site with the highest occupancy was adjacent to residues G5 and A6 in the catalytic core. This Tb ion was the only one observed in the soak experiment. One of the two binding sites with lower occupancy identified in the cocrystallization experiment

A. L. Feig and O. C. Uhlenbeck, Department of Chemistry and Biochemistry, University of Colorado, Boulder, CO 80309, USA.

W. G. Scott, Department of Chemistry, Indiana University, Bloomington, IN 47405, USA.

\*To whom correspondence should be addressed. E-mail: olke.uhlenbeck@colorado.edu

was located near G16.4 and the loop terminating stem III, whereas the other was located along stem I. Terbium ions at both of these sites bind outside the core of the hammerhead and also make outer-sphere contacts with symmetry-related RNA molecules in the crys-

tal, suggesting that they may not be present in solution. It is therefore likely that the observed inhibition of cleavage by Tb(III) results from metal binding to the site adjacent to G5.

An expanded view of this binding site

shows that Tb(III) interacts with the base-pairing face of G5 in the uridine turn of the catalytic core (Fig. 3B). At this resolution, the electron density of the Tb ion cannot be distinguished from that of the water molecules bound to it (23). The site lies within a substantial concave pocket along the RNA surface, but, unlike most RNA metal-binding sites, no phosphate residues are present nearby. On the basis of the distances between the center of the Tb(III) ion and nearby atoms (Table 2), we infer that Tb(III) interacts with the base-pairing face of a guanosine (G5), with water-mediated contacts to the adjacent adenosine and 2'-hydroxyl groups of nearby riboses. The closest contact is 3.8 Å from the N1 atom of this guanosine, a distance too great to represent an inner-sphere bond with the RNA. The crystallographic conditions, however, include 1.8 M Li<sub>2</sub>SO<sub>4</sub>; at such high ionic strength, the details of the coordination environment might be slightly altered from those observed with normal buffered aqueous solutions.

Although the competition data suggest that a Mg(II) ion binds near the core Tb(III) site, crystallography reveals only a weak electron-density peak in this region (7). Gel-mobility data, however, have shown that a Mg(II)-dependent conforma-

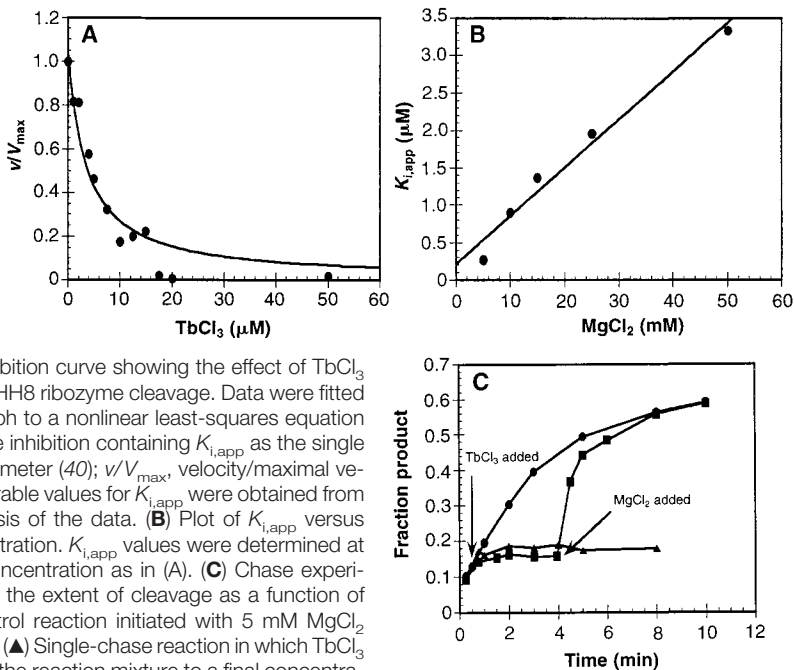


**Fig. 2.** (A) Inhibition curve showing the effect of  $TbCl_3$  on the rate of HH8 ribozyme cleavage. Data were fitted by Kaleidagraph to a nonlinear least-squares equation for competitive inhibition containing  $K_{i,app}$  as the single unknown parameter (40);  $v/V_{max}$ , velocity/maximal velocity. Comparable values for  $K_{i,app}$  were obtained from a Dixon analysis of the data. (B) Plot of  $K_{i,app}$  versus  $MgCl_2$  concentration.  $K_{i,app}$  values were determined at each  $Mg(II)$  concentration as in (A). (C) Chase experiment showing the extent of cleavage as a function of time. (●) Control reaction initiated with 5 mM  $MgCl_2$  with no chase. (▲) Single-chase reaction in which  $TbCl_3$  was added to the reaction mixture to a final concentration of 10  $\mu M$  at the time indicated. (■) Double-chase reaction treated as the single-chase reaction with the exception that, at the time indicated, 1 M  $MgCl_2$  was added to give a final concentration of 100 mM.

**Fig. 3.** (A)  $|F_{obs} - F_{calc}|$  difference map contoured at  $5\sigma$  showing the position of the Tb(III) ions. The crystals were grown as previously described (7) but in the presence of 2 mM  $TbCl_3$ . Details of the data collection and refinement are given in Table 1. The substrate strand is shown in orange and the ribozyme strand in blue. Residues in green have the closest contacts to the core Tb(III) ion, which is shown in red. The arrow indicates the cleavage site. This figure was prepared with the program O (41). (B) Stereoview of the core Tb(III) binding site. This figure was prepared with InsightII (BIOSYM).

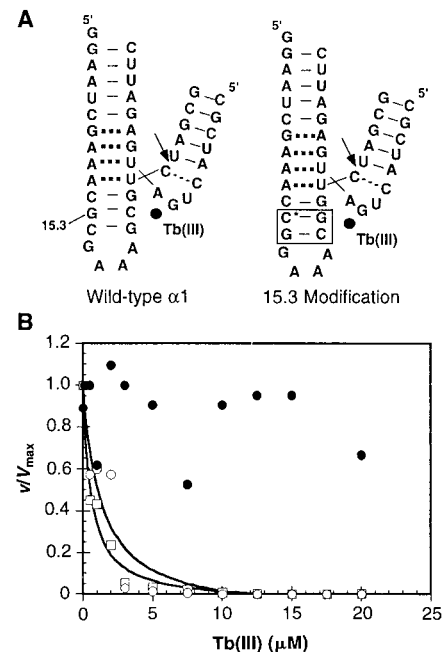
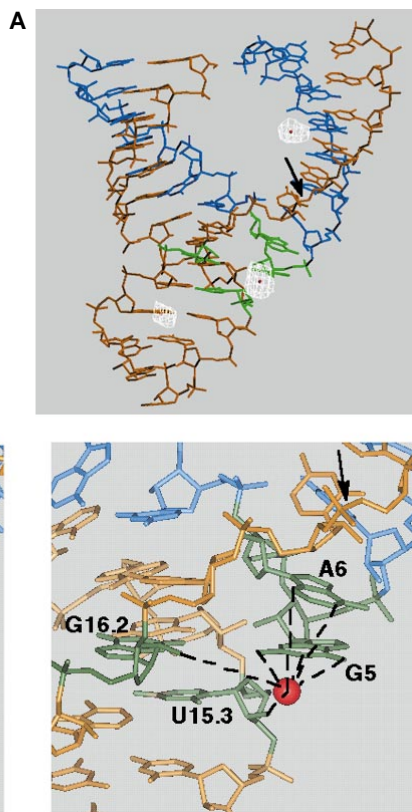


**Fig. 4.** (A) Secondary structures of the constructs used for 2'-amino modification at position 15.3. The boxed residues were subjected to base-pair inversion relative to the wild-type sequence to place a cytosine, for which the protected 2'-amino phosphoramidite was available (C\*), at this position. (B) Inhibition curves show the effects of Tb(III) on HH $\alpha 1$  (□), 15.3 2'-amino (○), and 15.3 2'-acetamido (●) substrates in the presence of 10 mM  $Mg(II)$  and 50 mM Pipes (pH 6.5) at 25°C.

tional isomerization of the hammerhead requires G5 (24, 25). In addition, crystal-soaking experiments have identified a Mn(II) ion 2.1 Å from the Tb(III) site (7). Because Mn(II) can often replace Mg(II) in RNA crystal structures (26–29), we propose that a Mg(II) ion also binds at a site close to that observed for Tb(III). Although the general binding site has remained constant, the shift in the coordination mode may reflect the preference of Tb(III) to bind to single-stranded guanosine nucleotides (30).

Confirmation of the binding site for the inhibitory Tb(III) ion was provided by experiments in which a 2'-amino-modified substrate was incorporated at position 15.3 of an HHα1-based construct (Fig. 4A). This position is located ~6.7 Å from the metal-binding site. The 15.3 2'-amino group was then converted to an acetamide by coupling an acetate to the primary amine with 1-(3-dimethylaminopropyl)-3-ethylcarbodiimide (EDC) (31). The relative cleavage rates of the 2'-amino and 2'-acetamido substrates are 156 and 73%, respectively, of that of the unmodified species; however, the 15.3 2'-acetamido-modified RNA was no longer sensitive to the presence of Tb(III) up to 20 μM in the cleavage reaction mixture (Fig. 4B). Under similar conditions, both the wild-type and 2'-amino substrates were completely inactive due to Tb(III) inhibition [Tb(III)  $K_{i,app}$  values:  $0.57 \pm 0.03$ ,  $1.3 \pm 0.4$ , and  $>20$  μM for the wild-type, 2'-amino, and 2'-acetamido substrates].

The core Tb(III)-binding site is located adjacent to G5. This residue lies in the center of the four-nucleotide uridine turn that has been suggested to constitute part of the catalytic pocket (6). Mutation of G5 to A (32) or deleting it entirely (33) reduces the cleavage rate by four orders of magnitude, identifying this residue as critical for catalysis. Even the incorporation of inosine or 2-amino purine at this position results in a reduction in rate by a factor of 100 (4). Nevertheless, in the crystal structure, this guanosine base is 10 Å from the cleavage site and does not make direct hydrogen-bonding contacts to the rest of the RNA molecule. For this reason, it has been proposed that G5 might undergo rearrangement on approach to the transition state (4, 34). It is thus possible that metal ions binding in this vicinity act as switches that help to control catalytic activity.

At least two hypotheses can be proposed to explain the inhibition of the hammerhead ribozyme by Tb(III). Whereas both assume that the tighter binding Tb(III) ion acts by displacing a weaker binding Mg(II) ion, they suggest different roles for the Mg(II) ion during hammerhead catalysis. In the first scenario, the Mg(II) ion assists in forming the transition-state structure, perhaps by maintaining a particular orientation between G5 and the nearby stem III. The essential functional groups on G5 would then be needed to correctly position the Mg(II) ion. Because of its different coordination preferences and size,

Tb(III) may not be able to maintain this structure properly. In the second proposal, the Mg(II) ion must be released in order for G5 to participate in the transition-state structure. By binding much more tightly than Mg(II) at this site, Tb(III) acts by locking the ribozyme in the crystallographically observed conformation. This latter hypothesis implies that not all of the Mg(II) ions that bind the hammerhead help to promote catalysis; instead, some may either inhibit catalysis or have no effect at all.

The synthetic modification experiments begin to address the issue of which model most accurately represents the function of the Mg(II) ion bound to G5. The bulky group on the 2' position of 15.3 renders the hammerhead resistant to Tb(III) inhibition, presumably by sterically blocking the binding site. However, the rate of cleavage of this modified RNA in the presence of Mg(II) is similar to that of the unmodified species. If the Mg(II) ion that normally binds to G5 is also unable to interact with this modified hammerhead, it must not be essential for the transition-state structure. Whereas these data appear to refute the first mechanism presented above for Tb(III) inhibition, further studies will be required to show definitively that this Mg(II) is indeed displaced by the 2'-acetamido modification. The proposal that this metal ion is released before the transition state is achieved is consistent with the mechanistic data currently available, but leaves open the actual role of G5 in hammerhead ribozyme catalysis.

We studied the binding of the physiological divalent metal ion Mg(II) to the hammerhead ribozyme by competition with a nonphysiological trivalent ion, Tb(III). This approach allowed us to propose a role for the Mg ion that binds adjacent to G5. It binds to the ground-state conformation and is released before the transition state is achieved, possibly in such a way that it helps to control this process. Such experiments, however, are limited neither to the

**Table 1.** Summary of crystallographic data. Data were collected with 0.870 Å x-rays on a 30-cm MAR imaging plate detector at 100 K. Crystals were rapidly frozen in the reservoir solution containing 20% (v/v) glycerol as a cryoprotectant. Data were processed with Mosflm (35) and CCP4 (36), and the model was refined with X-PLOR version 3.1 (37). The final model of the TbCl<sub>3</sub> cocrystal contains all residues of the hammerhead ribozyme and three Tb(III) ions.

	Native*	TbCl <sub>3</sub> cocrystal
Synchrotron x-ray source	X12C†	9.6‡
Wavelength (Å)	1.400	0.870
Resolution (Å)	43.0–3.0	35.8–2.9
Total reflections	23,810	30,459
Unique reflections	7003	7810
Redundancy of data	3.4	3.9
Mean $I/\sigma(I)$ (overall data)	15.9	6.75
Completeness (%)	85.4	97.7
Space group	P3 <sub>1</sub> 21	P3 <sub>1</sub> 21
Unit cell a (Å)	64.56	65.54
Unit cell c (Å)	136.29	138.08
$R_{scale}$ §	0.068	0.052
$R$ factor	0.216	0.256
$R_{free}$ ¶	0.265	0.302
	<i>Root-mean-square deviations</i>	
Bond lengths (Å)	0.007	0.015
Bond angles (degrees)	1.1	2.2
Dihedral angles (degrees)	13.0	14.9
Planar angles (degrees)	1.5	1.1

\*Reference (7). †Brookhaven National Laboratory NSLS. ‡Daresbury Laboratory SLS. § $R_{scale} = \sum |I_i - \langle I_i \rangle| / \sum |I_i|$ , where  $I_i$  is the intensity value of an individual measurement and  $\langle I_i \rangle$  is the corresponding mean value. Summations run over  $i$  measurements of all imaging plates. || $R$  factor =  $\sum |F_{obs} - F_{calc}| / \sum |F_{obs}|$ , where  $F_{obs}$  and  $F_{calc}$  are the observed and calculated structure factors, respectively. ¶ $R_{free}$  is the cross-validation  $R$  factor computed for the test set of reflections (10% of total).

**Table 2.** Selected contacts between the metal ion adjacent to G5 and the RNA.

		MnCl <sub>2</sub> soak*	TbCl <sub>3</sub> soak	TbCl <sub>3</sub> cocrystal
Occupancy		0.5	0.2	0.4
$B$ factor (Å <sup>2</sup> )†		38.7	50.9	52.7
		<i>Contacts (Å)‡</i>		
G5	N1	3.4	4.5	3.8
	N2	4.1	4.8	3.9
	O6	4.0	5.1	4.7
A6	N1	4.1	5.7	5.0
	N3	5.3	6.1	6.8
U15.3	O2'			6.7
G16.2	O2'	5.7	6.1	5.9
U16.1	O2'	4.1		

\*Reference (7). †isotropic temperature factor. ‡Mean error on these distances is  $\pm 0.3$  Å.

hammerhead ribozyme nor to these metal ions. Any RNA for which an assay is available to monitor metal exchange can, in principle, be used. Folded RNAs provide complex surfaces to which different metal ions can bind, with each site having its own specificity. The binding site observed with one competitor, therefore, may not necessarily be the same as that observed with another. Because few RNAs have been crystallographically characterized, the current challenge is to develop structural or functional methods to identify unique metal ion sites on these complex folded RNA structures.

## REFERENCES AND NOTES

- R. H. Symons, *Trends Biochem. Sci.* **14**, 445 (1989).
- C. C. Sheldon, A. C. Jeffries, C. Davies, R. H. Symons, in *Nucleic Acids and Molecular Biology*, F. Eckstein and D. M. J. Lilley, Eds. (Springer-Verlag, Berlin, 1990), vol. 4, pp. 227–242.
- A. C. Forster, A. C. Jeffries, C. C. Sheldon, R. H. Symons, *Cold Spring Harbor Symp. Quant. Biol.* **52**, 249 (1987).
- D. B. McKay, *RNA* **2**, 395 (1996).
- H. W. Pley, K. M. Flaherty, D. B. McKay, *Nature* **372**, 68 (1994).
- W. G. Scott, J. T. Finch, A. Klug, *Cell* **81**, 991 (1995).
- W. G. Scott, J. B. Murray, J. R. P. Arnold, B. L. Stoddard, A. Klug, *Science* **274**, 2065 (1996).
- D. E. Ruffner and O. C. Uhlenbeck, *Nucleic Acids Res.* **18**, 6025 (1990).
- G. Slim and M. J. Gait, *ibid.* **19**, 1183 (1991).
- M. Koizumi and E. Ohtsuka, *Biochemistry* **30**, 5145 (1991).
- J. A. Piccirilli, J. S. Vyle, M. H. Caruthers, T. R. Cech, *Nature* **361**, 85 (1993).
- R. G. Kuimelis and L. W. McLaughlin, *J. Am. Chem. Soc.* **117**, 11019 (1995).
- L. B. Weinstein, B. C. N. M. Jones, R. Cosstick, T. R. Cech, *Nature* **388**, 805 (1997).
- J. M. Wolfson and D. R. Kearns, *Biochemistry* **14**, 1436 (1975).
- D. E. Draper, *Biophys. Chem.* **21**, 91 (1985).
- W. D. Horrocks Jr., *Methods Enzymol.* **226**, 495 (1993).
- Substrate oligonucleotides were prepared with an Applied Biosystems ABI-394 automated synthesizer by standard phosphoramidite methodology [N. Usman, K. K. Ogilvie, M. Y. Jiang, R. J. Cedergren, *J. Am. Chem. Soc.* **109**, 7845 (1987)]. Standard deprotection protocols were used, after which the oligomers were purified by electrophoresis on 20% polyacrylamide gels, eluted into 0.5 M ammonium acetate, and precipitated with ethanol. Concentrations were determined by measuring absorbance at 260 nm. The ribozyme strands were prepared by T7 transcription from synthetic DNA template oligonucleotides as previously described [J. F. Milligan, D. R. Groebe, G. W. Witherell, O. C. Uhlenbeck, *Nucleic Acids Res.* **15**, 8783 (1987)]. These RNA molecules were purified by electrophoresis on 15% polyacrylamide gels and eluted as described above. Radiolabeled substrate was prepared by 5' end-labeling with <sup>32</sup>P according to standard methods [T. Maniatis, E. F. Fritsch, J. Sambrook, *Molecular Cloning: A Laboratory Manual* (Cold Spring Harbor Laboratory Press, Cold Spring Harbor, NY, 1982)].
- Saturating concentrations of ribozyme (500 nM) and trace <sup>32</sup>P-labeled substrate were annealed for 90 s at 90°C in 50 mM Pipes (pH 7.5), and then allowed to cool to 25°C. Reactions were initiated by adding MgCl<sub>2</sub> to the appropriate final concentration. When Tb(III) was present, it was added concomitantly with the Mg(II). Reactions were quenched by diluting a 10-μl portion of the reaction mixture into 20 μl of stop buffer (100 mM EDTA, 7 M urea, 1 × tri-borate-EDTA, 0.1% bromophenol blue, 0.1% xylene cyanol, 0.1% orange G). Reaction products were analyzed by electrophoresis on denaturing 20% polyacrylamide gels and quantitated with a Molecular Dynamics Phosphorimager and ImageQuant software. Pseudo-first order rate constants were calculated with Kaleidagraph (Synergy Software) from nonlinear least-squares fitting of plots of the fraction product [product/(product + substrate)] versus time. For extremely slow reactions, initial rates derived from linear fits of the same plots were used to estimate the rate constants. Protracted reactions (>4 to 6 hours) in the presence of Tb(III) were problematic because of nonspecific degradation of the RNA under the conditions used for kinetic analysis (22). Standard 1-hour time courses showed no substantial degradation. Reactions were usually performed in triplicate and the data averaged to give the observed rate constant. Errors are reported as standard deviations of the mean from replicate experiments.
- K. J. Hertel, D. Herschlag, O. C. Uhlenbeck, *Biochemistry* **33**, 3374 (1994).
- B. Clouet-d'Orval and O. C. Uhlenbeck, *RNA* **2**, 483 (1996).
- The K<sub>1,app</sub> for the Tb(III) interaction with HH8 at 10 mM MgCl<sub>2</sub> was 0.9 ± 0.2 μM.
- A. L. Feig and O. C. Uhlenbeck, unpublished data.
- Typically, inner-sphere water molecules would be located 2.42 ± 0.01 Å from the Tb(III) ion [E. Moret, F. Nicolò, J.-C. G. Bünzli, G. Chapuis, *J. Less-Common Metals* **171**, 273 (1991)].
- G. S. Bassi, N.-E. Møllegaard, A. I. H. Murchie, E. von Kitzing, D. M. J. Lilley, *Nature Struct. Biol.* **2**, 45 (1995).
- G. S. Bassi, A. I. H. Murchie, D. M. J. Lilley, *RNA* **2**, 756 (1996).
- A. Jack, J. E. Ladner, D. Rhodes, R. S. Brown, A. Klug, *J. Mol. Biol.* **111**, 315 (1977).
- J. H. Cate and J. A. Doudna, *Structure* **4**, 1221 (1996).
- J. H. Cate *et al.*, *Science* **273**, 1678 (1996).
- S. R. Holbrook and S.-H. Kim, *Biopolymers* **44**, 3 (1997).
- D. P. Ringer, B. A. Howell, D. E. Kizer, *Anal. Biochem.* **103**, 337 (1980).
- 2'-Acetamido modification of RNA has been previously described [C. Hendrix *et al.*, *Biochem. Biophys. Res. Commun.* **210**, 67 (1995); C. Hendrix *et al.*, *Nucleic Acids Res.* **23**, 51 (1995)]; however, we adopted a postsynthetic approach in which a 2'-amino substrate RNA was treated with 25 mM acetic acid and 25 mM EDC in 200 mM MES buffer (pH 6.5) for 30 min at 37°C. An additional 10 μl of 250 mM EDC was then added to the 100-μl reaction mixture and allowed to react for 30 min. The reaction product was isolated by precipitation with ethanol and examined by matrix-assisted laser desorption/ionization-time-of-flight mass spectroscopy, with 3-hydroxypicolinic acid as a matrix. On the basis of this analysis, the reaction was >90% complete, with no residual starting material evident in the spectrum.
- D. E. Ruffner, G. D. Stormo, O. C. Uhlenbeck, *Biochemistry* **29**, 10695 (1990).
- A. Peracchi, L. Beigelman, N. Usman, D. Herschlag, *Proc. Natl. Acad. Sci. U.S.A.* **93**, 11522 (1996).
- A. Peracchi, L. Beigelman, E. Scott, O. C. Uhlenbeck, D. Herschlag, *J. Biol. Chem.* **272**, 26822 (1997).
- Mosfilm, version 5.4.1; A. G. W. Leslie, Medical Research Council Laboratory of Molecular Biology, Cambridge, UK.
- Collaborative Computational Project Number 4, *Acta Crystallogr. D* **50**, 760 (1994).
- X-PLOR, version 3.1; A. T. Brünger, Yale University (1988–92), Harvard University (1987).
- K. J. Hertel *et al.*, *Nucleic Acids Res.* **20**, 3252 (1992).
- M. J. Fedor and O. C. Uhlenbeck, *Biochemistry* **31**, 12042 (1992).
- I. H. Segel, *Enzyme Kinetics* (Wiley, New York, 1993).
- T. A. Jones and M. Kjeldgaard, *O—The Manual: Manual for O Version 5.8.1*. (Uppsala University, Uppsala, Sweden, 1992).
- Supported by NSF (CHE-9504698 to A.L.F.) and NIH (GM-36944 to O.C.U.). We thank L. Behlen and J. Murray for preparing several of the synthetic oligonucleotides; E. Jabri, S. Cohen, and A. Klug for discussions; S. Price for help with data collection at Daresbury Laboratory; and W. Pieken for the 2'-amino cytosine phosphoramidite. Coordinates from the Tb(III) cocrystallization experiment have been deposited in the Nucleic Acids Database (NDB ID URX067).

21 July 1997; accepted 11 November 1997

## Quantitation of Transcription and Clonal Selection of Single Living Cells with β-Lactamase as Reporter

Gregor Zlokarnik, Paul A. Negulescu, Thomas E. Knapp, Lora Mere, Neal Burres,\* Luxin Feng, Michael Whitney, Klaus Roemer, Roger Y. Tsien†

Gene expression was visualized in single living mammalian cells with β-lactamase as a reporter that hydrolyzes a substrate loaded intracellularly as a membrane-permeant ester. Each enzyme molecule changed the fluorescence of many substrate molecules from green to blue by disrupting resonance energy transfer. This wavelength shift was detectable by eye or color film in individual cells containing less than 100 β-lactamase molecules. The robust change in emission ratio reveals quantitative heterogeneity in real-time gene expression, enables clonal selection by flow cytometry, and forms a basis for high-throughput screening of pharmaceutical candidate drugs in living mammalian cells.

Biological specificity is mediated by the precise and selective regulation of gene expression in response to intrinsic developmental programs and extrinsic signals. To

understand the regulation of gene expression, it is essential to use an assay of high sensitivity and fidelity that reports expression at the level of the single living cell.